Available online at www.sciencedirect.com

SciVerse ScienceDirect

Scripta Materialia 69 (2013) 586–589

Scripta MATERIALIA

www.elsevier.com/locate/scriptamat

Small-scale plasticity: Insights into dislocation avalanche velocities

Robert Maaß,[a,*] Peter M. Derlet[b] and Julia R. Greer[a,c]

[a] *California Institute of Technology, 1200 E California Blvd, Pasadena, CA 91125-8100, USA*
[b] *Paul Scherrer Institut, Condensed Matter Theory, 5232 Villigen PSI, Switzerland*
[c] *Kavli Institute of Technology, California Institute of Technology, Pasadena, CA 91125, USA*

Received 6 May 2013; revised 2 July 2013; accepted 3 July 2013
Available online 15 July 2013

We report direct measurements of displacement jump velocities in deforming nano- and microcrystals. These velocities exhibit large scatter and no correlation with plastic strain, crystal size or applied stress. Statistical analysis for the displacement jump velocities shows a cubic power-law decay, with a shoulder at low velocities. Our results indicate that the collective motion of dislocations in the deforming crystals is dominated by statistical fluctuations within the internal stresses, rather than by a mobility law that depends on the externally applied stress.

Keywords: Plasticity; Dislocations; Micromechanics; Size effect

Micro- and nanosized single crystals exhibit marked differences in plastic flow behaviour as compared to equivalent bulk crystals. For example, small-scale crystals follow a power-law strengthening of type $\sigma \sim d^{-n}$, where d is the characteristic length scale of the sample (i.e. diameter) and n a power-law exponent on the order of ~0.6 for face-centred cubic (fcc) metals [1,2]. This trend has been observed consistently for the dislocation-containing fcc [3–7] and body-centred cubic (bcc) [8,9] nano- and microsized single crystalline metals fabricated by a variety of techniques. Another characteristic feature of plastic deformation of metals at the nano- and micron-scales is the discontinuous progression of flow, where the stress–strain data contains multiple displacement bursts when loaded in compression or tension. The first indications of such phenomena were observed decades ago in Zn single crystals [10]. This burst-ridden plasticity was explained through the movement of dislocations, which were triggered sporadically within the evolving and unstable existing dislocation network on the crystallographic plane oriented most favourably for slip.

Today, measurements on deforming micro- or nanocrystals possess high enough resolution to precisely determine the magnitude of most displacement jumps with a sub-nanometer resolution. This has allowed the exploitation of the statistical signature of discrete plastic flow in both fcc and bcc crystals [11–13]. It has been shown, for example, that the probability of a certain displacement magnitude to occur follows a power-law distribution over at least two orders of magnitude, which is a typical signature of a scale-free process, similar to the crackling noise of magnetic domain switching or plate techtonics [14]. The analysis of displacement burst statistics usually involves setting a threshold on the minimum displacement burst to filter out the real displacement burst from the background noise of the recorded data. This is commonly done by differentiating the displacement data with respect to time and to define a rate threshold, above which the data is considered a detectable event. Despite the low data acquisition rates (DAR) of between 5 and 25 Hz in many measurements [5,11,13], such a rate thresholding is able to define those events that later are investigated on the basis of the high-resolution displacement signal, but it is not capable of capturing the true displacement rate of the individual glide events, commonly referred to as dislocation avalanches.

In this work, we combined the high displacement resolution of a Hysitron Triboscope with a DAR of 7 kHz to investigate the displacement jump velocities of deforming [0 0 1] -oriented cylindrical Au micro- and nanocrystals with diameters of 300 nm, 500 nm, 2 μm and 5 μm. The crystals were prepared via focused ion-beam milling from a gold single crystal following an established methodology [3,4,15]. The vertical sample

* Corresponding author. Now at: Institute of Materials Physics, University of Göttingen, 37077 Göttingen, Germany. Tel.: +1 49 1728256898; e-mail: robert.maass@ingenieur.de

1359-6462/$ - see front matter © 2013 Acta Materialia Inc. Published by Elsevier Ltd. All rights reserved.
http://dx.doi.org/10.1016/j.scriptamat.2013.07.005

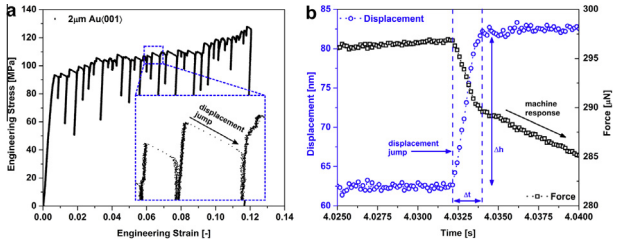

Figure 1. (a) Compressive stress–strain data of a 2 μm diameter sample, with the inset displaying two zoomed-in displacement jumps; (b) displacement and force signal as a function of time during a displacement jump.

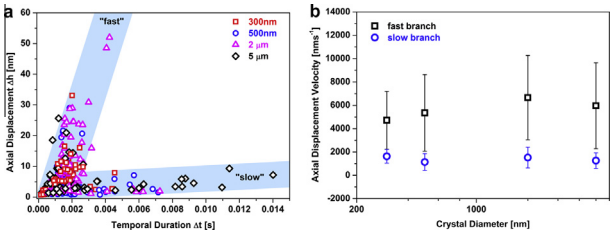

Figure 2. (a) Axial displacement jump magnitudes, Δh, and their corresponding temporal durations, Δt, for all investigated sample sizes. Two distinct data clusters are schematically indicated as fast and slow. (b) Axial displacement jump velocity for the fast (square symbols) and slow (circular symbols) branches vs. crystal diameter.

tapering, which is commonly associated with this technique, was measured to be ~1.16°, and the average aspect ratio was ~3. Microcompression testing in displacement rate control was performed with a steering unit that allows to record more than 200,000 data points per test. Two conical diamond tips, with flattened ends of 9 and 15 μm diameter, were used for compression at a nominally constant applied strain rate of 5×10^{-3} s^{-1}.

The stress–strain data of a typical compression experiment for a 2 μm crystal is shown in Figure 1a. At a stress between 90 and 100 MPa, excessive plastic elongation sets in, which is the typical strength range for such crystals. Multiple stress drops are discernible during post-elastic flow. The inset highlights a zoomed-in data segment of two successive displacement jumps and reveals that a portion of the stress drop occurred during the forward surge, which is partly a result of the elastic stress release in the load–frame–sample assembly. At the end of a displacement jump, the stress rapidly drops by more than several tens of megapascals. This drop in the applied stress is a result of the displacement controlling steering system of the nanoindenter. Subsequent reloading is linear elastic.

Figure 1b displays the displacement and the force signal as a function of time during a typical displacement jump. The simultaneous occurrence of a displacement jump and a rapid force drop in the time interval Δt is followed by a more gradual decrease in the force, $-\Delta F/\Delta t$. This gradual force reduction is caused by the nanoindenter retracting the compression tip to its prescribed position. Such a correction of the faster-than-prescribed displacement represents one of the earmarks of conducting nanomechanical experiments on small-scale crystals under a nominally constant displacement rate. The subsequent response is primarily elastic, as evidenced by the virtually full overlap of the stress decrease and the subsequent reloading segment (Fig. 1a). The high DAR is critical in such experiments to record and identify the proper shape and duration of each displacement jump. We focused on the measureable time interval, Δt, and the extent of displacement, Δh, selected on the basis of a displacement jump threshold of 0.8 nm. This value is significantly higher than the nominal displacement noise floor (0.2 nm) of the Hysitron Triboscope.

Analysis of at least 90 individual events per set of equivalent-sized samples revealed a range of spatio-temporal bursts, displayed in Figure 2a. Larger displacement jumps correlate with longer durations. The data appears to be naturally binned into two different regimes of clustered axial displacements and durations. These clusters do not correlate with sample size.

The two branches become indistinguishable at the lower end of both axes, i.e. for shorter time durations and displacements. Hence, the data points below the function $\Delta h = k\Delta t$ ($k \approx 2500$) were grouped as "slow" and those above were marked as "fast". We derived a corresponding averaged axial displacement velocity, $\Delta h/\Delta t$, for each sample size and each branch. The results are summarized in Figure 2b, which reveals a lack of any correlation between the axial displacement velocity and the sample size for both the "fast" and the "slow" branches. Figure 2b also contains a two orders of magnitude range in the axial displacement velocities. The velocity invariance with respect to sample size was found to pervade over a wide range of "slow" and "fast" bin separation criteria. The data displayed in Figure 2b indicates that the averaged axial displacement velocity, and thus the dislocation avalanche velocity, during bursts was independent of the applied stress between 28 and 450 MPa for all sample sizes. Figure 3 summarizes the axial displacement jump velocity as a function of applied plastic strain, ε. Similarly to the trend depicted in Figure 2b, no apparent correlation between plastic strain and the recorded axial displacement velocity exists. This finding is valid for both speed bins (Fig. 2a), and is compatible with the notion of little change occurring within the dislocation structure during plastic flow [16,17].

The validity of these results hinges upon addressing several critical questions. Firstly, are there potential instrumental concerns that may affect the measured invariances with respect to sample size, applied stress and plastic strain? Secondly, if this is not the case, what link can be made to the motion of the group of dislocations that is fundamentally giving rise to the measured displacement jump?

It is plausible that the data points in Figure 2b represent a forward velocity limit inherently imposed by the nanoindenter – a scenario where the sample may slip faster than the movement of the indenter. Estimating the possible acceleration and maximum velocity of the tip–spring assembly yields values of the order found here, not allowing the exclusion of a device limit. However, several arguments also suggest that this is not the case: (i) a purely device-limited result would be expected to yield a tight distribution of data because it represents a machine characteristic. The spread in the data

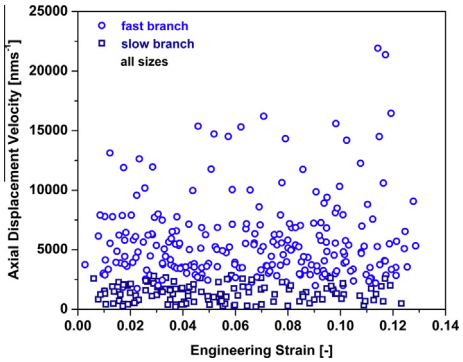

Figure 3. The axial displacement jump velocities for all investigated sample sizes and both the slow and fast branches as a function of applied plastic strain.

measured here is greater than two orders of magnitude. (ii) Given a device limit and the observed large scatter, some events must naturally occur at faster velocities than the machine is capable of. Such a loss followed by the re-establishment of contact would be discernible in the data shown in Figure 1b. This is not observed. Further, it is not clear how a dislocation avalanche would move without any applied force, given that dislocation motion is over-damped where inertia plays no role. (iii) The clustering of the data into two distinct correlations between Δh and Δt indicates that it cannot be ascribed to a velocity cap of the forward surging indenter tip. (iv) If the data generated in our experiments were a reflection of the device properties only, it would be reasonable to expect a sample size dependence. This is because the forces that trigger the avalanches are significantly sample size dependent, and thus the elastic energy released during an avalanche – and therefore the tip velocity – would be strongly dependent on size. This is also not observed. Whilst more instrumental investigations are required to better understand the device–sample interplay, our line of reasoning suggests that the data measured in the course of this work is representative of the underlying dislocation activities and crystallographic slip. While the absolute magnitude of each displacement burst may be affected by the machine–sample assembly, we believe that the relative trends described here are related to the mean velocity of the collectively moving dislocations during the intermittent plastic flow in the crystals.

It is reasonable to assume that the internal microstructure within these crystals is based on a dislocation network, and that the intermittent plasticity is mediated by the irreversible rearrangements within this network. With this assumption, any localized internal slip should scale roughly with the volume of the sample. Such an approach was developed by Eshelby [18,19], where a strain increment, $\Delta\varepsilon$, was proportional to the slipped area, ΔA, within the sample:

$$\Delta\varepsilon \propto \frac{\Delta A \times b}{d^2 \times h}$$

where b is the magnitude of the Burgers vector, d is the sample diameter and h is the sample height. The proportionality constant would be a function of the nature of the loading geometry and the orientation of the slipped area. The average axial displacement velocity for an event is then $v_{ad} = h\Delta\varepsilon/\Delta t$, which implies that, on average, the axial displacement velocity is proportional to the rate of the internally slipped area. The overall ΔA may be represented by a number of characteristic microscopic irreversible rearrangements, ΔA_0, whose number is set by a volumetric dislocation density, ρ. These rearrangements occur within a plastic volume, $d^2\Delta d$, where Δd is the thickness of a typical slip band, such that $\Delta A = \rho d^2 \Delta d \Delta A_0$. The average axial displacement velocity can then be calculated as:

$$v_{ad} \propto \rho \Delta d b \times \frac{\Delta A_0}{\Delta t}$$

The scaling of the plastically deformed volume with the diameter squared is motivated by the lack of the scatter dependence on the pillar diameter (Fig. 3) and the observation that dislocations exit the pillar leaving slip-steps in their wake. If the microscopically slipped area corresponds to a characteristic length of a mobile dislocation segment, l, then $\Delta A_0/\Delta t = l v_d$, where v_d corresponds to an average dislocation avalanche velocity. Thus the mean velocity v_{ad} can be expressed as:

$$v_{ad} \propto \rho \Delta d l b \times v_d$$

This equation represents a simple proportionality relation between the average velocities of the axial displacement and of the dislocation avalanches. Such an approach is in the spirit of that of Hoffmann et al. [20], who expressed the growth rate of a slip-step height, which is equivalent to the resolved value of v_{ad}, as being proportional to $v_d b/x_d$, where x_d (here equal to $(\rho\Delta d l)^{-1}$) is the average distance travelled by a group of edge dislocations. An analogous approach was used in slip-line cinematography for investigations of the slip-step growth normal to the surface [21]. In the same studies, the group dislocation velocity was determined along the slip-line growth direction, where it could be derived directly from the propagating front. The use of $v_{ad} \propto \rho \Delta d l b \times v_d$ in the present context is limiting because of the significant scatter of the axial velocity data, which likely arose from the variations in the dislocation avalanche velocity v_d and/or the internal length scale x_d (or l).

Modern dislocation dynamics simulations have provided important insights into small-Such methods are at the forefront of understanding the underlying

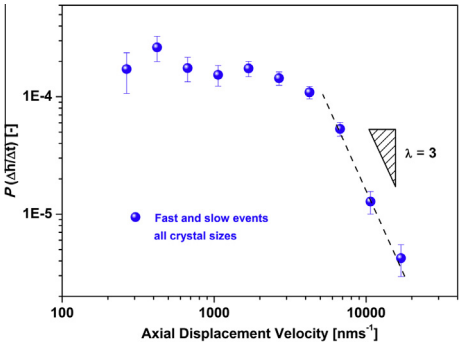

Figure 4. Displacement jump velocity distribution of all measured data. The dashed line indicates a cubic decay ($\lambda = 3$), whereas fitting the higher-end data yields a power-law exponent of 2.9 ± 0.2.

three-dimensional dislocation mechanisms and plasticity at small scales [22], and can also be used in a simplified way to study intermittent dislocation activity [23]. Important to the present work is the recent dislocation dynamics investigation of the dislocation velocity distribution, $P(v)$, associated with the avalanches of the discrete plastic events [24]. These authors reported a dislocation velocity distribution that scales as a power law $P(v) \sim v^{-\lambda}$ with $\lambda \approx 3$, which saturated at low velocities.

Under the assumption that the present scatter seen in the axial displacement velocities is predominantly due to variations in the average dislocation velocity v, the data of Figure 3 is binned logarithmically over all strains and pillar sizes (applied stresses) to obtain an experimentally derived dislocation avalanche velocity distribution. Figure 4 displays the obtained distribution and reveals a remarkable similarity to the simulation derived distribution of Ispanovity et al. (see fig. 4 of Ref. [24]), as well as with theoretical predictions [25]. Indeed, Figure 4 reveals both the saturation at low velocities and an approximate power law at higher velocities that has a cubic decay, as indicated by the dashed line. Fitting the high velocity data in this work yields an exponent of $\lambda \approx 2.9 \pm 0.2$ (Fig. 4).

With such good agreement between the experiments and simulations, the lack of correlation between the scatter in the axial displacement velocity and pillar size implies a similar lack of dependence on the applied stress, and may now be easily understood. In computer simulations the glide velocity of dislocations is typically assumed to be over-damped and proportional to an acting Peach–Koehler force. Ispanovity et al. [24] demonstrated that the lower v part of the dislocation velocity distribution was weakly dependent on the applied stress (see Fig. 5 in Ref. [24]). This indicates that it is not the applied stress but, rather, the internal stress landscape and its dynamics upon changes of the dislocation network that dominates the underlying mobility law. Our experiments convey the absence of dependence of dislocation avalanche velocity on the externally applied stress, extending even to the higher v part of the distribution, well within the cubic decay regime. Following the results in Ref. [24], the slow branch in Figure 2a seems likely to correspond to the quiescent dislocation avalanche state, whereas the fast branch can be linked to the avalanche state.

In summary, we investigated the displacement jump velocity during intermittent flow of nano- and microcrystals. The data can be binned into two distinct clusters of displacement jump velocities, which may be linked to a quiescent and an avalanche state of dislocation motion. Experiments revealed significant scatter within the data, with the concurrent lack of correlation between the displacement burst velocity and plastic strain or crystal size. Such a size independence of the displacement jump velocity translates into its independence on the applied stress over a range of ca. 400 MPa. Since it is believed that a displacement jump corresponds directly to a dislocation avalanche (moving group of dislocations), such a stress independence was unexpected in the light of the original work on dislocation velocities [26]. The resulting velocity distribution is found to agree with recent dislocation dynamics simulations [24] and theory [25], supporting the physical validity of our experimental results. Our findings suggest that, in the size regime of the studied crystal sizes, the underlying dislocation mobility is primarily determined by the internal stress field landscape and its dynamics, originated by the evolving dislocation network, rather than by an externally applied stress-driven mobility law. Even though the data is well in line with a modern viewpoint on plasticity, we acknowledge that further efforts need to be dedicated to the understanding of potential instrumental issues.

R.M. gratefully acknowledges the financial support of the Alexander von Humboldt foundation, and his host G.M. Pharr for valuable discussions. J.R.G. is thankful for the financial support of the Office of Naval Research (ONR Grant N000140910883).

[1] M.D. Uchic et al., Annu. Rev. Mater. Sci. 39 (2009) 361.
[2] J.R. Greer, J.T.M. De Hosson, Prog. Mater. Sci. 56 (2011) 654.
[3] J.R. Greer et al., Acta Mater. 2005 (1821) 53.
[4] C.A. Volkert, E.T. Lilleodden, Philos. Mag. 86 (2006) 5567.
[5] C.P. Frick et al., Mater. Sci. Eng. A 489 (2008) 319.
[6] R. Maass et al., Acta Mater. 57 (2009) 5996.
[7] R. Maass et al., Small 2012 (1869) 8.
[8] J.R. Greer et al., Mater. Sci. Eng. A 493 (2008) 21.
[9] S. Shim et al., Acta Mater. 57 (2009) 503.
[10] R.F. Tinder, J.P. Trzil, Acta Metall. 21 (1973) 975.
[11] D.M. Dimiduk et al., Science 312 (2006) 1188.
[12] S. Brinckmann et al., Phys. Rev. Lett. 100 (2008) 155502.
[13] M. Zaiser et al., Philos. Mag. 88 (2008) 3861.
[14] M.C. Miguel et al., Nature 410 (2001) 667.
[15] R. Maass et al., Mater Sci. Eng. A 524 (2009) 40.
[16] D.M. Norfleet et al., Acta Mater. 56 (2008) 2988.
[17] R. Maass, M.D. Uchic, Acta Mater. 60 (2012) 1027.
[18] J.D. Eshelby, J. Appl. Phys. 25 (1954) 255.
[19] J.D. Eshelby, Proc. R. Soc A – Math. Phys. Eng. Sci. 241 (1957) 376.
[20] U. Hoffmann et al., J. Microsc. 203 (2001) 108.
[21] H. Neuhäuser, in: F.R.N. Nabarro (Ed.), Dislocations in Solids, vol. 6, North-Holland Publishing Company, Amsterdam, 1983, p. 319.
[22] P.M. Derlet, R. Maass, Model. Simul. Mater. Sci. Eng. 21 (2013) 035007.
[23] P.M. Derlet et al., MRS Bull. 34 (2009) 184.
[24] P.D. Ispanovity et al., Phys. Rev. Lett. 105 (2010) 085503.
[25] M. LeBlanc et al., Phys. Rev. E 87 (2013) 13.
[26] W.G. Johnston, J.J. Gilman, J. Appl. Phys. 30 (1959) 129.